

Facile Approach in Fabricating TiO₂/organic Functional Coatings

Yansheng Zheng^{1,2,*}, Chunyan Mo², Falong Wang², Qian Mo²

¹Lushan College of Guangxi University of Science and Technology, Liuzhou 545616, Guangxi, PR China

²College of Biological and Chemical Engineering, Guangxi University of Science and Technology, Liuzhou 545006, Guangxi, PR China

*E-mail: mochunyan1990@163.com

Received: 10 September 2015 / Accepted: 13 October 2015 / Published: 4 November 2015

Nano-scale TiO₂ and micro-scale PTFE were used to fabricate a series of coatings on steel substrate through a facile approach. Scanning electron microscopy, thermal analysis, contact angle analyzer and electrochemical tests were obtained to describe the coatings' surface morphologies, optimum temperature, wetting properties and anti-corrosion performances, respectively. The results indicated that the optimum temperature of these coatings was 200 °C. Under this temperature, rich composite interface structures would form on the coating surface. Further more, the as-formed coating would exhibit the best super-hydrophobic with water contact angle as 154.5° and excellent anti-performance with the biggest E_{corr}, β_a and β_b as -0.65 V, 0.13 V/dec, 0.25 V/dec, respectively, the smallest j_{corr} as 4.45×10⁻⁵ A.cm⁻² and the largest diameter as shown.

Keywords: Facile approach; nano-scale; micro-scale; super-hydrophobic; anti-corrosion performance

1. INTRODUCTION

In recent years, the solid surface with super-hydrophobic (water static contact angle exceeding 150° and water sliding angle less than 10°) has attracted considerable interest thanks to its special advantages and potential prospects in both fundamental research and practical applications.[1] Many studies found that the combination of hierarchical micro/nano dual roughness and low surface energy were two key factors for the super-hydrophobic of such solid surfaces.[2,3] Therefore, creating suitable texture with micro/nano rough structure on hydrophobic materials has become a significant method to fabricate super-hydrophobic surface as well as modifying a rough substrate with low surface energy.

It's generally known that nanotechnology is the science of materials at the molecular or subatomic level and its application prospect is very extensive. Nowadays, the application of this fast-evolving technology to super-hydrophobic scientific research has drawn much attention.[4] Nano-particles such as TiO₂ have been applied extensively onto metal substrates and subsequent hydrophobic modification with fluorinated silane[5] or stearic acid[6] due to their non-toxicity, low price, high availability biocompatibility and cost-effectiveness. For instance, Jiang et al.[7] used both micro-arc oxidation technique and self-assembling reaction to fabricate functional TiO₂ patterns with super-hydrophobicity, good anti-corrosion and high hemocompatibility on biomedical Ti-6Al-4V alloys. The results indicated that the water contact angle between water and the as-formed patterns arrived at 153.39°. what's more, to be compared with those of uncoated, these patterns' corrosion resistance values increased obviously by raising one order of magnitude. Nishimoto et al.[8] made it possible to quickly fabricate superhydrophobic–superhydrophilic samples without photomask through a new formation method. According to the research, the TiO₂-based printing samples were fabricated on an anodized aluminum plate followed by surface modification of TiO₂ film, patterning of aqueous ink by the ink-jet technique, UV light irradiation and water washing. Furthermore, the wettability plates were reusable and applicable to offset printing. Given above, there is no doubt that the incorporation of super-hydrophobic properties into TiO₂ device surface can widen its application area.

Increased attention has recently been paid to Polytetrafluoroethylene(PTFE) which can be easy to manufacture and typically possess excellent properties including low surface energy and adhesion, high temperature and biological stability, excellent resistance to chemical reagents and degradation.[9] It is commonly thought to be a good choice as a versatile fluoropolymer material widely used to fabricate super-hydrophobic surfaces due to such advantages. The contact angle (CA) between commercially available PTFE and water droplet usually reaches 104-108°.[10,11] Moreover, considering surface energy, the descending order of -CH₂- > -CH₃- > -CF₂- > -CF₂H- > -CF₃- may help us to learn more about super-hydrophobic scientific studies, especially on fluorine-containing materials.[12] Dong et al.[13] got several films by changing the amount of PTFE micro-powder in the mixed solution (mix polyvinylidene fluoride with polytetrafluoroethylene) from 0 wt.% to 12 wt.%, the results showed that the contact angle between the films and water are range from 130.4° to 152.2°. Zheng et al.[14] fabricated super-hydrophobic and heat-resistant membranes on glass plate by sol-gel method. SiO₂ sol and PTFE emulsion were used as raw materials and γ -Glycidoxypropyl trimethoxysilane was used to increase the compatibility between the two former phases so to reduce the phase separation. It was observed that the as-prepared membranes had good hydrophobic with average water contact angle of 156° and sliding angle of 6°.

In this letter, we fabricated a series of coatings on the basis of organic (PTFE emulsion) and inorganic (TiO₂ nanoparticles) through sol-gel method. Steel coupon and stearic acid were used as metal substrate and surface modifier, respectively. The thermal analysis, surface morphologies and wetting properties of the as-formed coatings were observed as well anti-corrosion performances. The results demonstrated that all the covered-specimens showed better anti-corrosion performance than the bare steel, and, the composite coating exhibited the best super-hydrophobic when the heat-treatment temperature was at 200 °C.

2. EXPERIMENTAL DETAILS

2.1 Sample preparation

First of all, orderly add TiO_2 (5 g, purchased from Shanghai jiang titanium dioxide chemical products co., LTD with average particle size 10-30 nm) and stearic acid (0.4 g, purchased from Guangdong Shantou Xinlong chemical plant) that was well dissolved in 40 mL of ethanol into 40 mL of DI water under magnetic stirring for more than 2h at 80 °C followed by adding suitable Sodium Dodecyl Benzene Sulfonate (SDBS, obtained from Shantou guanghua chemical plant). Then, the amount of 2.4 g PTFE emulsion (60 wt.%, 1.2 g.mL⁻¹, obtained from Guangzhou Songpo Chemical Company with average particle size 0.2-0.3 um) and 1 mL ammonia solution ($\text{NH}_3\cdot\text{H}_2\text{O}$) were slowly joined as well as 1 mL silane coupler (G-570). After that, the reaction mixture's pH was adjusted to 5.0 by 2 M acetic acid. What's more, it was kept stirring for another 3 h and aged at room temperature for 8 h until a homogeneous white viscous liquid was obtained. Finally, uniform hybrid coatings were formed on steel substrate after dip-coating process and heat treatment with 130, 170, 200, 230 and 270°, respectively. The schematic illustration of fabricating composite coatings was showed as Fig. 1.

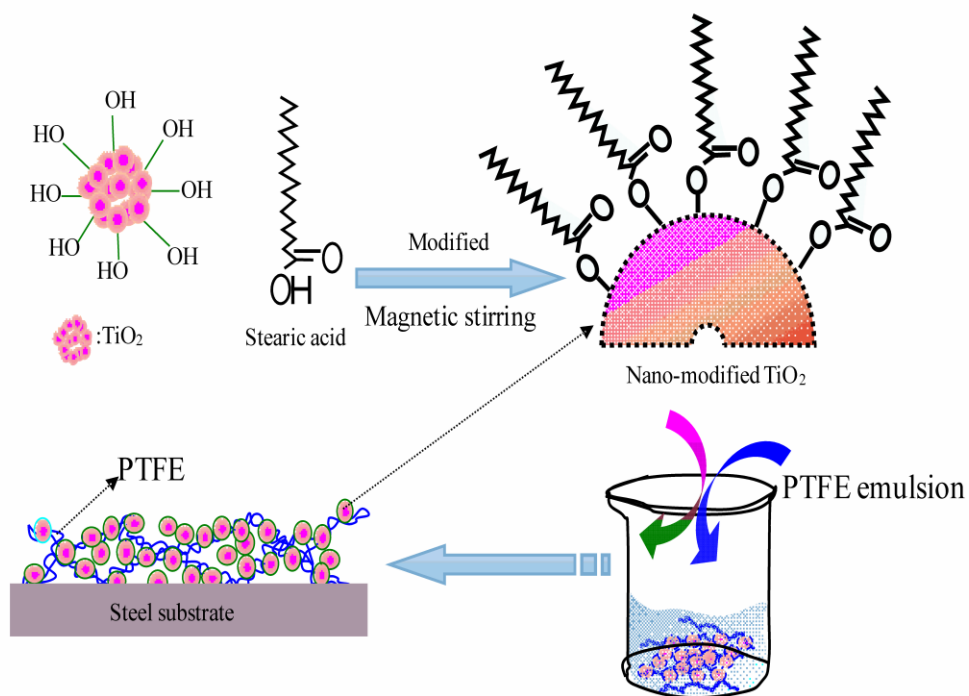


Figure 1. The schematic illustration of fabricating composite coatings

2.2 Characterization

The water contact angles of as-prepared coatings and their surface morphology structures were characterized by sessile drop method (Dataphysics OCA20) and digital scanning electron microscopy (SEM, S-3400N) respectively. The stability of composite powders were tested with thermo gravimetric

analysis (TG, Netzsch STA449F3A-1103-M). Electrochemical methods including polarization curve measurement and alternating current impedance were measured by CHI 660D electrochemical analyzer to characterize the corrosion of composite coatings at room temperature. All specimens were immersed in 3.5 wt. % NaCl electrolyte solution for 36 h with a scanning rate of 5 mV/s, the potential range was from -1.4 V to -0.1 V. The tests were performed by a three-electrode method, which consists of a working electrode, a reference electrode and an auxiliary electrode.

3. RESULTS AND DISCUSSION

3.1 Thermal analysis and hydrophobic studies

As we all know, the hydrophobicity of the solid surface is determined by both the chemical composition and microstructure of the surface.[15-17] What's more, the heat-treatment temperature has certain kinds of relationships with these two factors.[18]

In order to understand the effect of the heat-treatment temperature on the wettability of the as-prepared surface coverage, we fabricated a series of coatings under different heat-treatment temperatures such as 130, 170, 200, 230 and 270 °C for 1 h. According to Fig. 2 and Tab.1, We can see that the CA and surface appearance on coating changed significantly with the increase of temperature. Further more, the CA attained maximum (CA = 154.5°) when the heat-treatment temperature was 200 °C. However, the CA reduced apparently either as the temperature of below 170 °C or exceed 230 °C. This may due to the change of organic molecules, resulting to the change of the surface structure. Fig. 3 presents the thermal analysis curves (TG-DTG) of the TiO₂/PTFE particles when the heat-treatment temperature was 200 °C. The quality was not changed obviously when the temperature was below 200 °C, This may due to the molecular-level physical adsorption or desorption behaviors of the surface chemical reagents and water. The high heat resistance of PTFE up to 260 °C may account for this as well.[19] In addition, The obvious mass-loss rate of composite particles achieved at about 18% when the temperature was between 250 °C and 800 °C especially at about 550 °C, which meant the composite particles were suffering from thermal damage. This mainly attributed to the complete oxidative decomposition of organic materials like the methyl groups, stearic acid and PTFE molecular chain.

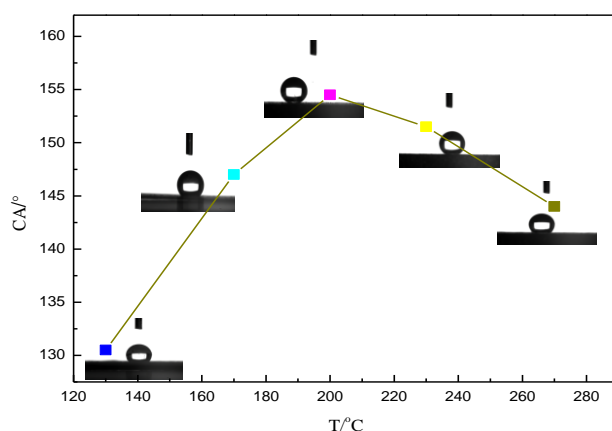
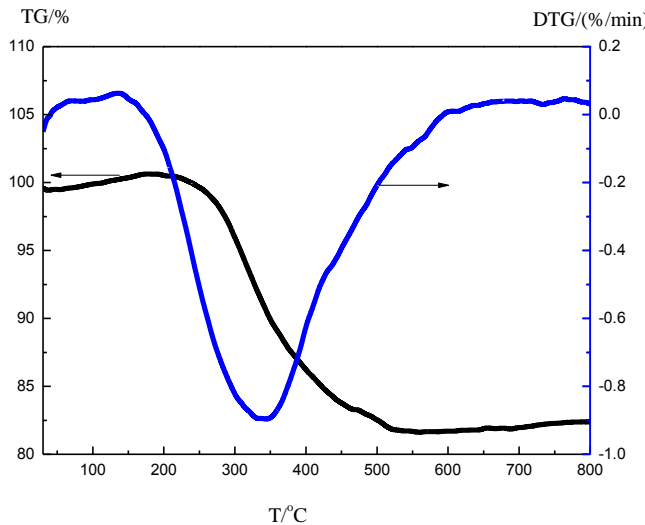


Figure 2. Effect of heat treatment on WCA

Table 1. Effect of the heat-treatment on CA of coating

Sample	Heat-treatment temperature/ °C	CA/°	Coating appearance
1	130	130.5	no cracks
2	170	147.0	no cracks
3	200	154.5	no cracks
4	230	151.5	A few of cracks
5	270	144.0	A lot of cracks

**Figure 3.** Thermal analysis curves of TiO₂/organic composite particles

3.2 Surface morphology

The surface morphology is one of the most critical factors on the hydrophobicity of the solid coating.[20,21]

In our case, we use nano-sized TiO₂ (Fig. 4a) and micro-level PTFE (Fig. 4b) as raw materials. The results showed that the TiO₂ powders were well dispersed on PTFE surface with a narrow size distribution. Besides, the PTFE exhibited homogeneous networks with good cross-linking and unique hierarchical air-cushion structures. After reacted with each other, the surface morphology of composite particles became more abundant (Fig. 4c). To be specific, the air-cushion structures were filled with nano-sized TiO₂ powders and a large fraction of air were trapped within the grooves among such micro/nano dual structure, which can dramatically increase the surface roughness of the composite coating and prevent the coating from being corroded by corrosive species.[22]

Theoretical basis are important for us to understand the behaviors of the hydrophobized TiO₂/PTFE coatings. According to the Cassie-Baxter model[23] (shown as Fig.5) and the mechanism of anti-corrosive[24] (shown as Fig. 6), the coatings that with good hydrophobicity always have both low surface energy and hierarchical micro/nano dual structures[25]. Of the two, the micro/nano dual structures are closely related to gas-liquid-solid composite interface that can trap the air into “ravines” between “peaks” easily to form an “air protection shield” when it’s in corrosive solution, which is important to prevent the corrosion medium penetrating into the substrate directly. The configuration of the Cassie-Baxter model can be described as the following equation[26-28]:

$$\cos\theta_{CB} = (1-f) \cos\theta - f \quad (1)$$

Where f is the fraction of air in contact with water, θ_{CB} is the contact angle of a water droplet on a rough surface while θ is on a smooth surface. Both θ_{CB} and θ are in the range of 0-180° where the cosine value will monotonically decreases as the angle increases. In our case, the CA value on the best as-prepared composite coating (θ_{CB}) and bare smooth steel surface(θ) are 154.5° and 76°, respectively. It is easy to know from Eq. (1) that the f value is 0.916, which indicates that the air contacted with water occupies about 91.6% of the contact area between water and micro/nano structure. The final image of the hydrophobic properties of TiO₂/PTFE coating sintered at 200 °C is showed in Fig. 7 as well as the uncoated steel surface.

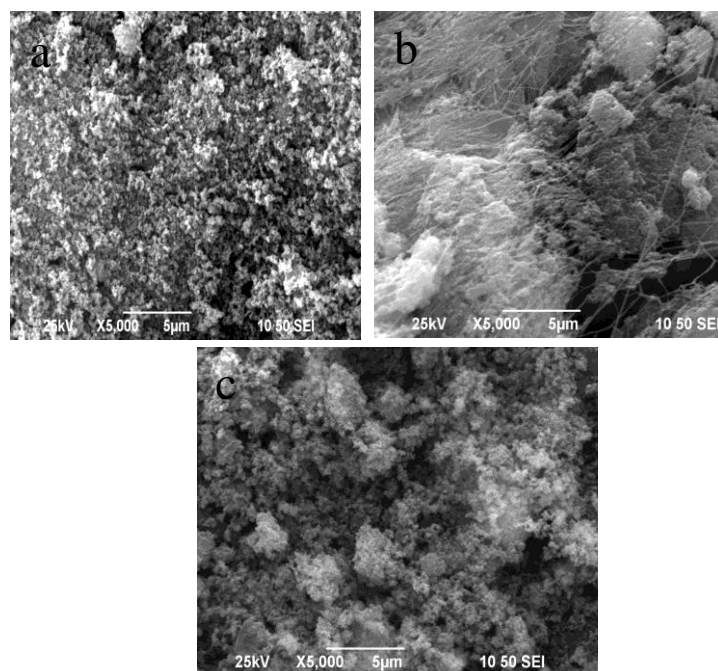


Figure 4. Morphologies of samples:(a) modified TiO₂ particles, (b) pure PTFE, (c) TiO₂/PTFE particles sintered at 200 °C

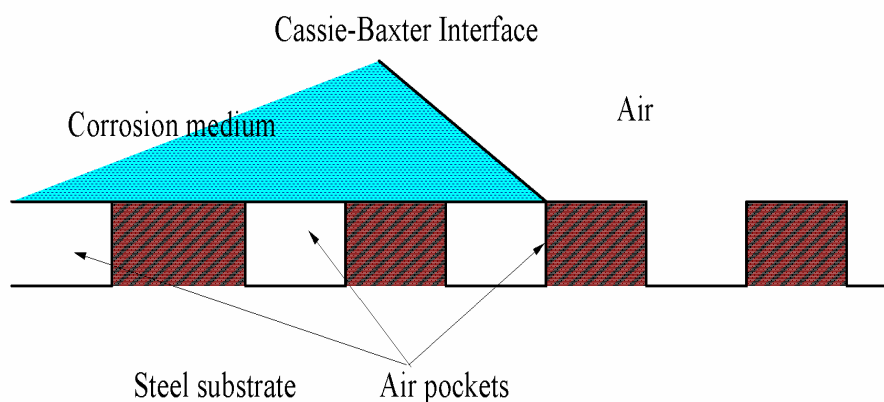


Figure 5. Schematic diagram of Cassie-Baxter model

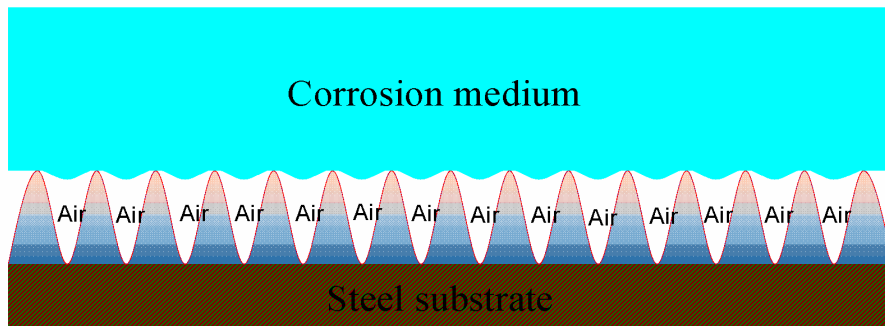


Figure 6. Anti-corrosive mechanism of TiO_2 / organic composite coating

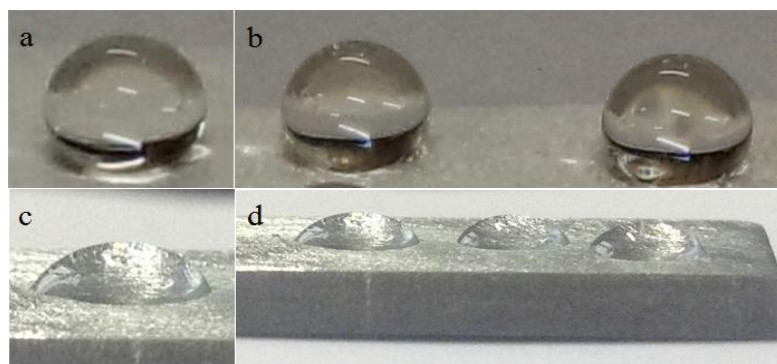


Figure 7. The water droplets on the specimens' surfaces:(a-b) TiO_2 /PTFE specimen sintered at 200 °C, (c-d) uncoated steel specimen

3.3 Electrochemical measurements

In order to evaluate the anti-corrosion behaviors of the as-prepared coatings, electrochemical measurements like Potentiodynamic polarization measurement and Electrochemical impedance measurement (EIS) are described. Corrosion potential (E_{corr}) and Corrosion current density (j_{corr}) calculated from extrapolation of these curves to their point of intersection are given as the parameters to evaluate the anti-corrosion performance of coatings, anodic Tafel constants (β_a) and cathodic Tafel constants (β_c) are given in Tab. 2 as well. Generally, a high E_{corr} or a low j_{corr} corresponds to a large corrosion resistance a good anti-corrosion performance.[29] According to the former study, we choose six different samples (bare steel, modified TiO_2 , pure PTFE, composite TiO_2 /PTFE treated with 170, 200, 230 °C) to be measured. The results are showed in Fig. 8, Tab. 2 and Fig.9 for comparison.

Fig. 8 shows the Tafel plots of uncoated steel substrate and a series of coated samples. In particular, Tafel curve (a), (b), (c) is the bare steel substrate, modified TiO_2 and pure PTFE, respectively. The next series of specimens denoted with (d), (e) and (f) represent the composite coating(TiO_2 / PTFE) treated with 170, 230 and 200 °C. As shown in Fig. 8. Both Tafel constants (β_a and β_c) and the corrosion potential (E_{corr}) of all coated-specimens are more positive while their corrosion current density (j_{corr}) are decreasing obviously compared to the uncoated one. All calculated values (E_{corr} , β_a , β_c , j_{corr}) of specimens coated with pure TiO_2 and PTFE are very close, which may due to their single component, leading to poor protection against NaCl solution. In

addition, the E_{corr} (β_a , β_c) value of specimens coated with TiO_2 / PTFE coating exhibit better anti-corrosion performance than pure PTFE coating and modified TiO_2 coating. This may be a result of the good dispersion of TiO_2 particles on PTFE, when the nano-particles uniformly distribute and has a good combination with micro-scale organic material, the composite coating will exhibit better properties than that of simple material.[30]

Combine with the computational results (corrosion potential (E_{corr}) and corrosion current density (j_{corr})) in Tab. 2. We can easily see that the bare steel has the smallest E_{corr} , β_a , β_c as -0.95 V 0.13 V/dec, 0.25 V/dec, respectively. This may due to the direct contact with NaCl corrosive medium so there has little protection. More specifically, the sodium ions, chlorine ions, water molecules, oxygen and many other active ingredients may easily penetrate into the uncoated steel, resulting to no protection against the corrosion medium.[31,32] However, according to Tab. 2, the corrosion current density (j_{corr}) of the TiO_2 / PTFE specimen that heat-treated at 200 °C was $4.45 \times 10^{-5} A/cm^2$, which is, 1.62, 4.16, 7.57, 12.02, 131.69 times lower than that of 170, 230 °C, pure PTFE, modified TiO_2 and uncoated sample, respectively. The results may because of the changes of chemical compositions and the hydrophobicities of the coating surfaces.

Electrochemical impedance spectroscopy (EIS), which is investigated as well to evaluate the samples' anti-corrosion performance, confirms these results. Generally, we use the diameter of EIS curves to describe the specimens' anti-corrosion performance, larger the diameter is, better the anti-corrosion performance is.[33-35]

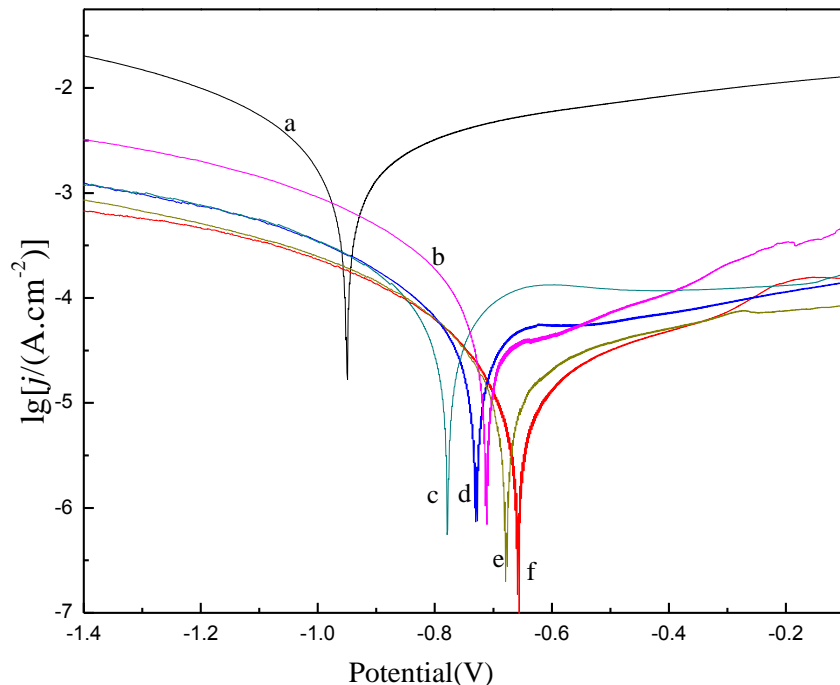


Figure 8. Tafel curves of steel specimens: (a) uncoated; coated with: (b) modified TiO_2 , (c) pure PTFE, (d) TiO_2 /PTFE sintered at 230 °C, (e) TiO_2 /PTFE sintered at 170 °C, (f) TiO_2 /PTFE sintered at 200 °C in 3.5% NaCl solution for 36 h

Fig. 9 shows the Nyquist plots of the specimens mentioned above. According to these results, both heat-treatment temperature and polymer material have prominent effects on the impedance of the specimens. We can easily observe that the coated specimens have larger diameter than the bare steel substrate, besides, the diameter of specimen that covered by TiO₂/PTFE treated with 200 °C is the largest. The reason is due to the coatings' rich gas-liquid-solid composite interface structures and good hydrophobicities. Moreover, combined with the air(acting as a barrier layer to the electrolyte by impeding its contact with steel substrate) trapped within pores, a secondary physical barrier is formed to protect the underlying steel from being corroded by the harmful ions such as sodium ions, chlorine ions and other corrosive ions.[36]

Table 2. Corrosion potentials and corrosion current densities of different samples

coating	corrosion potential/V	corrosion current density(A/cm ²)	β_a (V/dec)	β_b (V/dec)
Bare steel substrate	-0.95	5.86×10^{-3}	0.13	0.25
Nano modified TiO ₂	-0.71	5.35×10^{-4}	0.16	0.27
Polytetrafluoroethylene	-0.77	3.37×10^{-4}	0.15	0.33
TiO ₂ /PTFE (170 °C)	-0.68	7.21×10^{-5}	0.37	0.35
TiO ₂ /PTFE (200 °C)	-0.65	4.45×10^{-5}	0.42	0.45
TiO ₂ /PTFE (230 °C)	-0.73	1.85×10^{-4}	0.21	0.36

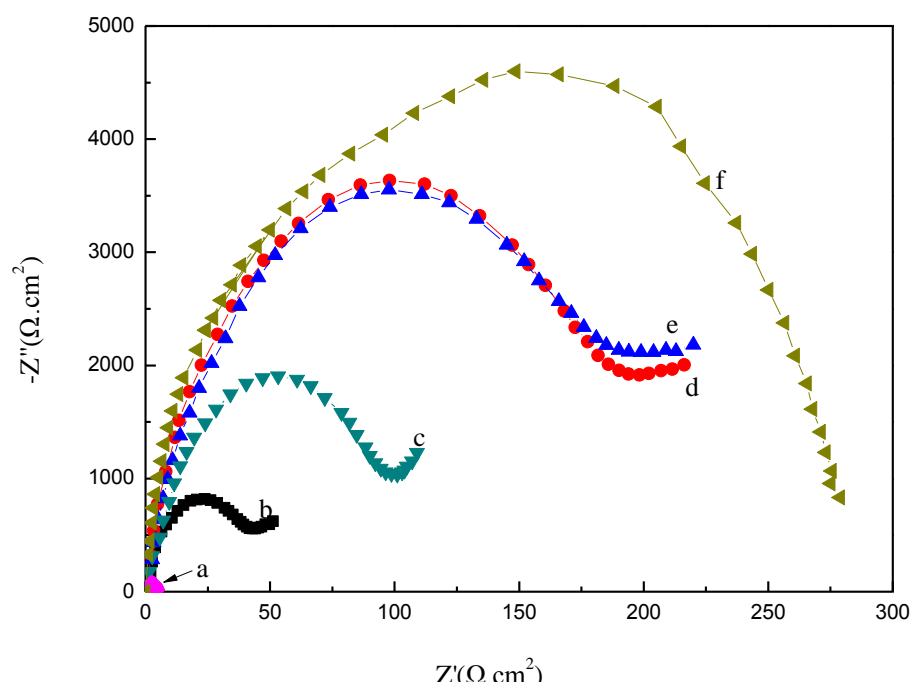


Figure 9. EIS curves of steel specimens: (a) uncoated; coated with: (b) modified TiO₂, (c) pure PTFE, (d)TiO₂/PTFE sintered at 230 °C, (e) TiO₂/PTFE sintered at 170 °C, (f)TiO₂/PTFE sintered at 200 °C in 3.5% NaCl solution for 36 h

4. CONCLUSION

In this letter, we prepared a series of coatings on steel substrate through a simple method. The nano-TiO₂ particles and micro-PTFE emulsion were used as raw materials in order to fabricate the micro-nano surface structure. Scanning electron microscopy and thermal analysis were obtained to describe both the surface structures and the best heat-treatment temperature of the coatings. Electrochemical tests including polarization method and Electrochemical impedance measurement were obtained to investigate the samples' anti-corrosion performances. The results showed that coating would have rich surface structure and best anti-corrosion performances (the biggest E_{corr}, β_a and β_b, the smallest j_{corr}, the largest diameter) when the heat-treatment temperature was at 200 °C, neither higher nor lower temperature was suit for the coating fabricating. Moreover, the contact angle analyzer proved the hydrophobicities of samples were different as the temperature changing, the biggest water contact angle achieved at 154.5, which was 178.5 positive shift compared to the bare steel sample at 76.

References

1. S. M. M. Ramos, J. F. Dias, B. Canut. *Journal of Colloid and Interface Science* 440 (2015) 133-139.
2. Y Chen, G Y Ou, F Li, T H Li. *Journal of Fluorine Chemistry* 175 (2015) 121-124.
3. J. Seyfi, S. H. Jafari, H. A. Khonakdar, G. M. M. Sadeghi, G. Zohuri, I. Hejazi, F. Simon. *Applied Surface Science* 347 (2015) 224-230.
4. S D Wang, B J Lin, C C Hsieh, C C Lin. *Applied Surface Science* 307 (2014) 101-108.
5. I. Bernagozzi, C. Antonini, F. Villa, M. Marengo. *Colloid and Surfaces A: Phsicochemical and Engineering Aspects* 441 (2014) 919-924.
6. M Liu, Y Qing, Y Q Wu, J Liang, S Luo. *Applied Surface Science* 330 (2015) 332-338.
7. Y Z Gao, Y W Sun, D M Guo. *Applied Surface Science* 314 (2014) 754-759.
8. S. Nishimoto, M. Becchaku, Y. Kameshima, Y. Shiroasaki, S. Hayakawa. *Thin Solid Films* 558 (2014) 221-226.
9. S. F. Toosi, S. Moradi, S. Kamal, S. G. Hatzikiriakos. *Applied Surface Science* 349 (2015) 715-723.
10. D. Jucius, V. Grigaliunas, M. Mikolajunas, A. Guobiene, V. Kopustinskas, A. Gudonyte, P. Narmontas. *Applied Surface Science* 257 (2011) 2353-2360.
11. D W Gong, J Y Long, P X Fan, D F Jiang, H J Zhang, M L Zhong. *Applied Surface Science* 331 (2051) 437-443.
12. H B Wang, E V Chen, X B Jia, L J Liang, Q Wang. *Applied Surface Science* 349 (2015) 724-732.
13. Z Q Dong, X H Ma, Z L Xu, W T You, F B Li. *Desalination* 347 (2014) 175-183.
14. Y S Zheng, Y He, Y Q Qing, Z H Zhou, Q Mo. *Applied Surface Science* 258 (2012) 9859-9863.
15. Y Qi, Z Cui, B Liang, R. S. Parnas, H F Lu. *Applied Surface Science* 305 (2014) 716-724.
16. T. Bharathidasan, S. V. Kumar, M. S. Bobji, R. P. S. Chakradhar, B. J. Basu. *Applied Surface Science* 314 (2014) 241-250.
17. C. K. Soz, E. Yilgor, I. Yilgor. *Progress in Organic Coating* 84 (2015) 143-152.
18. J. MacMullen, Z Y Zhang, J. Radulovic, C. Herodotou, M. Totomis, H. N. Dhakal, N. Bennett. *Energy and Buildings* 52(2012) 86-92.
19. M. Takachi, H. Yasuoka, K. Ohdaira, T. Shimoda, H. Matsumura. *Thin Solid Films* 517 (2009) 3622-3624.
20. C A Du, J D Wang, Z F Chen, D R Chen. *Applied Surface Science* 313(2014) 304-310.

21. Z X Gao, X L Zhai, F Liu, M Zhang, D L Zang, C Y Wang. *Carbohydrate Polymers* 128 (2015) 24-31.
22. D M Lv, J F Ou, M S Xue, F J Wang. *Applied Surface Science* 333 (2015) 163-169.
23. A. M. A. Mohamed, A. M. Abdullah, N. A. Younan. *Arabian Journal of Chemistry* 6 (2015) 749-765.
24. L B Feng, Y H Che, Y H Liu, X H Qiang, Y P Wang. *Applied Surface Science* 283 (2013) 367-374.
25. Z. Ghalmi, M. Farzaneh. *Applied Surface Science* 314 (2014) 564-569.
26. F. Henry, F. Renaux, S. Coppee, R. Lazzaroni, N. Vandecasteele, F. Reniers, R. Snyders. *Surface Science* 606 (2012) 1825-1829.
27. Z P Zuo, R J Liao, C Guo, Y Yuan, X T Zhao, A Y Zhuang. *Applied Surface Science* 331 (2015) 132-139.
28. H. B. Jo, J. Choi, K. J. Byeon, H. J. Choi, H. Lee. *Microelectronic Engineering* 116 (2014) 51-57.
29. Y H Fan, Z J Chen, J Liang, Y Wang, H Chen. *Surface & Coatings Technology* 244 (2014) 1-8.
30. K. Nakano, S. Akita, M. Yamanaka. *Colloid Polymer Science* 292 (2014) 1475-1478.
31. Y Liu, X M Yin, J J Zhang, S R Yu, Z W Han, L Q Ren. *Electrochimica Acta* 125 (2014) 395-403.
32. Z X She, Q Li, Z W Wang, C Tan, J C Zhou, L Q Li. *Surface & Coatings Technology* 251 (2014) 7-14.
33. I. L. Lehr, S. B. Saidman. *Progress in Organic Coatings* 76 (2013) 1586-1593.
34. T. Tuken, B. Yazic, M. Erbil. *Materials and Design* 28 (2007) 208-216.
35. H. Ozkazanc, S. Zor. *Progress in Organic Coatings* 76 (2013) 720-728.
36. Y L Shi, W Yang, X J Feng, Y S Wang, G R Yue. *Materials Letters* 151 (2015) 24-27.